

Autonomous and non-autonomous Shh signalling mediate the in vivo growth and guidance of mouse retinal ganglion cell axons

Cristina Sánchez-Camacho and Paola Bovolenta*

In non-mammalian vertebrates, the relatively homogeneous population of retinal ganglion cells (RGCs) differentiates and projects entirely to the contralateral side of the brain under the influence of sonic hedgehog (Shh). In mammals, by contrast, there are two different RGC types: the *Zic2*-positive ipsilateral projecting and the *Isl2*-positive contralateral projecting. We asked whether the axons of these two populations respond to Shh and if their response differs. We have also analysed whether midline- and RGC-derived Shh contributes to the growth of the axons in the proximal visual pathway. We show that these two RGC types are characterised by a differential expression of Shh signalling components and that they respond differently to Shh when challenged in vitro. In vivo blockade of Shh activity, however, alters the path and distribution mostly of the contralateral projecting RGC axons at the chiasm, indicating that midline-derived Shh participates in funnelling contralateral visual fibres in this region. Furthermore, interference with Shh signalling in the RGCs themselves causes abnormal growth and navigation of contralateral projecting axons in the proximal portion of the pathway, highlighting a novel cell-autonomous mechanism by which Shh can influence growth cone behaviour.

KEY WORDS: Growth cone, Morphogen, Chiasm, Boc, Transcriptional regulation

INTRODUCTION

The Hedgehog (Hh) family of secreted signalling proteins regulates pattern formation, proliferation, differentiation, cell migration and axon guidance in numerous organs (Fuccillo et al., 2006; Sanchez-Camacho et al., 2005), in many cases exerting more than one function on the same cell type. A prime example of these multiple activities of Hh is in the generation, differentiation and axon growth of vertebrate retinal ganglion cells (RGCs), which are responsible for transmitting visual information from the retina to the brain (Amato et al., 2004).

In non-mammalian vertebrates, FGF signalling triggers the onset of neurogenesis that generates the first neurons, the RGCs (Martinez-Morales et al., 2005). Newborn RGCs begin to express and release Shh, a member of the Hh family, which further propagates the differentiation wave, establishing a stable source of Shh within the eye (Esteve and Bovolenta, 2006). Once generated, RGCs extend an axon that exits the eye through the optic disc and navigates towards the ventral midline of the diencephalon, where axons from the two eyes meet to form the optic chiasm. In animals with panoramic vision, such as birds and fish, the entire axonal population from one eye projects to the contralateral side of the brain (Erskine and Herrera, 2007; Mason and Sretavan, 1997). Although Shh is strongly expressed along the ventral midline of the entire CNS, its expression is downregulated at the preoptic region just when retinal axons are approaching, whereas it is maintained at the chiasm borders (Trousse et al., 2001). Retroviral-mediated ectopic expression of Shh in the embryonic chick preoptic area impairs growth of the retinal fibres (Trousse et al., 2001). Similarly,

inappropriate expression of Shh at the optic chiasm, as observed in the *Pax2a* (*Pax2.1*; *noi*) zebrafish mutant, correlates with abnormal ipsilateral turning of RGC axons (Macdonald et al., 1995), indicating that local downregulation of Shh might be crucial for RGC midline crossing. Consistently, RGC growth cones respond with a reversible and re-inducible collapse upon repeated Shh applications, leading to the hypothesis that Shh diffusing from the chiasm borders might serve to restrict anteroposteriorly the growth of visual axons (Trousse et al., 2001). Furthermore, lowering or increasing Shh activity in the chick retina causes disorganisation of the fibre layer, indicating that adequate intraocular levels of the morphogen are also directly or indirectly required to direct RGC axon growth towards the optic disc (Kolpak et al., 2005).

Thus, RGCs are cells that secrete and perceive Shh, and their axons extend from the retina to the midline between two different Shh sources: the RGCs themselves and the preoptic area at the midline. Shh, however, is transported along the RGC axons (Traiffort et al., 2001), which presumably secrete the morphogen along their path, as detectable levels of Shh protein have been found in optic nerve extracts (Wallace and Raff, 1999). Consistent with an axonal release, pharmacological and genetic interference with RGC-derived Shh disrupts the development of a specialised group of glial cells at the optic disc (Dakubo et al., 2003; Morcillo et al., 2006), as well as the proliferation and migration of oligodendrocyte precursors (Merchan et al., 2007) and the differentiation of astrocytes in the optic nerve (Wallace and Raff, 1999). It is therefore logical to assume that RGC growth cones must be exposed to Shh even before reaching the midline.

Whether RGC-derived Shh contributes to axonal outgrowth remains unexplored. Likewise, whether mammalian RGC axons respond to Shh has not been analysed. This is a relevant question because there seem to be some species-specific differences between mice, fish and chick in Shh-mediated retinal differentiation (Esteve and Bovolenta, 2006), although the absence of contralateral projection in *Pax2*-null mice – in which, as in fish mutants, Shh is

Departamento de Neurobiología Molecular Celular y del Desarrollo, Instituto Cajal, CSIC and CIBER de Enfermedades Raras (CIBERER), Avda. Dr Arce 37, Madrid 28002, Spain.

*Author for correspondence (e-mail: bovolenta@cajal.csic.es)

abnormally expressed at the optic chiasm (Torres et al., 1996) – favours a conserved role for Shh at the chiasm midline. Furthermore, in mammals, both the specification and the midline behaviour of a subset of RGCs differ from those of fish and birds in that a proportion of axons originating in the temporal region of the retina do not cross the midline but instead project ipsilaterally, assuring binocular vision (Erskine and Herrera, 2007; Mason and Sretavan, 1997). Establishment of this ipsilateral projection requires the expression of *Zic2*, a zinc-finger transcription factor that is specifically expressed in ipsilateral but not contralateral projecting RGCs (I-RGCs and C-RGCs, respectively) (Herrera et al., 2003; Pak et al., 2004), and the activity of the EphB and ephrin B signalling proteins, which are localised to the I-RGC and chiasm, respectively (Williams et al., 2003). Whether *Zic2*-positive RGCs also express and sense Shh is unclear.

Here we have analysed whether Shh provides guidance information to the mouse RGC axons in their growth from the eye to the chiasm, and whether there are differences between the I- and C-RGC axonal populations, uncovering in the process differential non-autonomous (from the chiasm area) and cell-autonomous (from the RGC) functions of Shh.

MATERIALS AND METHODS

Animals

Embryos from C57BL/6J pregnant mice were collected between E13.5 and E18.5. *Shh::GFP^{Cre}/+* E14.5 and E16.5 embryos were also analysed (Harfe et al., 2004). Animals were handled according to Spanish (RD 223/88) and European (86/609/ECC) regulations.

In situ hybridisation and immunohistochemical procedures

Mouse embryos were fixed in 4% paraformaldehyde (PFA) in PBS (PFA/PBS) overnight at 4°C and sectioned by vibratome (40 µm) or cryostat (20 µm) in the coronal plane. Sections were hybridised with the following digoxigenin-labelled probes using standard protocols: *Shh*, *Ptc1*, *Ptc2*, *Hip1*, *Boc*, *Gli1*, *Gli2* and *Gli3*. Immunostaining of tissue sections and explant cultures was performed by standard protocols using the following antibodies: anti-Shh (5E1; ascitic liquid 1:200; DSHB), anti-*Zic2* (1:10,000), anti-*Isl2* (1:5000), anti-Gfap antiserum (Dako; 1:2000), anti-tubulin βIII (Tuj1; Tubb3) (Promega; 1:1000), anti-SSEA-1 (Fut4) (MC-480; 1:500), anti-Pax2 (Zymed Laboratories; 1:2000), anti-GFP (Molecular Probes; 1:1000) and Alexa Fluor 488- or 594-conjugated fluorescent secondary antibodies (Molecular Probes; 1:1000).

Retinal explants and collapse assays

Ventrotemporal (VT, predominantly containing I-RGCs) or dorsonasal (DN, containing C-RGCs) explants from E14.5 retinas were embedded in collagen gel matrix in the presence or absence of soluble or bead-immobilised Shh (1 µg/ml) as described (Trousse et al., 2001). In some cases, cyclopamine (10 µM, Toronto Research Chemicals, Toronto, Canada) was added to the medium. After 48 hours, explants were fixed in 4% PFA and stained with anti-Tuj1 antibody or Alexa Fluor 594-conjugated phalloidin (Molecular Probes; 1:40). Neurite outgrowth in the presence of different concentrations of Shh (0.25, 0.50, 1, 2, 4 and 6 µg/ml) was determined in DN and VT microexplants plated on glass coverslips coated with poly-D-lysine (10 µg/ml; Sigma) and laminin (10 µg/ml; Invitrogen) and grown for 24 hours as above. To determine Shh transport, VT and DN explants were cultured for 24 hours on glass coverslips (as above) and immunostained with the 5E1 antibody. Dorsal root ganglia and floor plate explants were used as negative and positive controls, respectively, for the immunostaining. For collapse assays, retinal explants established as above were treated after 24 hours with the following agents: Shh (1 µg/ml); SAG, a Smo agonist (0.3 µM); cyclopamine (5–10 µM); or the anti-Shh blocking antibody (5E1; 1:500, 1:1000). After 30 minutes, explants were fixed in 4% PFA and 11% sucrose at 37°C for 30 minutes, then stained with phalloidin. Cycloheximide (25 µM; Sigma), an inhibitor of protein synthesis, or actinomycin D (1 µg/ml),

a transcription inhibitor, was bath-applied 10 minutes before the addition of the above agents. Three independent experiments performed in quintuplicate were analysed for each condition.

Statistical analysis

Data were collected using the image analysis software AIS 6.0 (Analytical Imaging Station, Imaging Research, Ontario, Canada) and quantified using SPSS v15.0 (SPSS, Chicago, IL). To determine the extent of neurite outgrowth in collagen gel experiments, the area of the explant was subtracted from the total area occupied by Tuj1-immunopositive staining and normalised to explant size. Average neurite outgrowth was expressed as the mean ± s.e.m. in pixels. Statistical significance was calculated using an unpaired Student's *t*-test. For explants grown on glass coverslips, the area of outgrowth was determined using one-way ANOVA plus posthoc test (Dunnett test). For collapse assays, the area (µm²) and number of filopodia in growth cone confocal images (taken using a Leica TCS LS; Leica, Heidelberg, Germany) were evaluated using ImageJ 1.38 (NIH). Statistical significance was determined using the one-way ANOVA plus posthoc test (Dunnett test). Growth cones were classified into two different categories according to morphology: (1) 'spread' morphology, when the core of the growth cone was wide with lamellipodia and three or more filopodia; (2) 'collapsed' morphology, when the core of the growth cone was reduced with three or fewer filopodia. For each condition, the percentage of the growth cone belonging to one or other category was determined in three independent experiments performed in quintuplicate. Statistical differences were established using a contingency table with Fisher's exact test (treatment versus type of growth cone, significance level $\alpha=0.05$).

In vivo interference with Shh activity

Hybridomas secreting the anti-Shh 5E1 IgG, or control hybridomas [IgGs against the GAG viral capsid protein (DSHB)], were prepared as described (Merchan et al., 2007). Timed-pregnant E13.5 C57/BL6 mice were anaesthetised by inhalation (isoflurane 1–1.5% O₂) and 5–10 µl of a 2 × 10⁶ cells/ml suspension were injected directly into the amniotic sac. After 5 days, embryos were fixed and processed for immunostaining or DiI labelling. In other experiments, axons were visualised by retinal electroporation of a pCAGGS-EGFP construct (see below) after injection of the hybridoma into the amniotic sac.

DiI labelling of retinal projections

For unilateral anterograde labelling of retinal projections, small DiI crystals (Molecular Probes) were placed onto the optic nerve head of the right eye from fixed E18.5 embryos as described (Godement et al., 1987). For retrograde labelling, the preoptic area was exposed and a crystal of DiI, briefly dipped in Triton X-100, was inserted unilaterally in the initial portion of the optic tract. After 7–15 days at 23–37°C in PFA/PBS, the proximal visual pathway was analysed. The relative width of the optic chiasm was determined by measuring the distance from the rostralmost to the caudalmost DiI-labelled retinal axons at the chiasm midline using InStat 3.0 (GraphPad Software, San Diego, CA) and one-way ANOVA. In the case of retrograde labelling, contralateral and ipsilateral retinas were dissected and flat mounted. The extent of labelling was determined as the percentage of the total area that was occupied by retrograde DiI-labelled retinal axons.

In utero electroporation

Shh transduction in the mouse retina was blocked by in utero electroporation of a bicistronic vector containing *Ptc1^{Δloop2}* and a nuclear-targeted GFP (*Ptc1^{Δloop2}-IRES-GFPnls*), a construct that abrogates Shh-dependent activation of the signalling cascade (Briscoe et al., 2001). Nuclear GFP expression allowed determination of the position of electroporated cells. The trajectory of targeted axons was visualised by co-electroporation of pCAGGS-EGFP. E13.5 pregnant mice were anaesthetised and electroporated as described (Garcia-Frigola et al., 2007). Embryos were allowed to develop until E16.5.

Quantitative PCR

E16.5 retinas electroporated as described above were dissected and only GFP-positive tissue collected. Total RNA was extracted and purified following standard protocols (RNeasy Mini Kit, Qiagen). RNA was reverse-

transcribed using the High-Capacity cDNA Reverse Transcription Kit (Applied Biosystems). The quantitative PCR was performed using Power SYBR Green Master Mix following the manufacturer's protocol (Applied Biosystems) in a 25 μ l reaction mixture that contained 2 μ l of cDNA. Primers were designed using PrimerExpress (Applied Biosystems) with a melting temperature of 60°C. In all cases, the length of the amplicons was between 100 and 150 bp. Primer sequences are available upon request. The *Ptc1* 3' UTR primers were designed to detect only endogenous *Ptc1* levels after *Ptc1^{Loop2}* overexpression. The threshold cycle (C_t) values were measured by the ABI Prism 7500 Sequence Detection System. After an initial 2 minutes at 50°C and 10 minutes at 95°C, the thermal profile consisted of 40 cycles of 15 seconds at 95°C and 1 minute at 60°C. Triplicate samples from two independent experiments were measured and averaged. Expression levels were normalised to 18S rRNA levels and analysed by the unpaired Student's *t*-test.

RESULTS

Shh signalling pathway components are differentially expressed in the embryonic mouse I-RGCs and C-RGCs

Activation of the Shh pathway is initiated by ligand binding to the patched receptors [*Ptc1* (*Ptc1*), *Ptc2* (*Ptc2*)], which, through smoothened (*Smo*), activate an intracellular cascade leading to Gli-mediated transcriptional control of target genes. Additional surface regulators of the pathway include *Hip1* (Hedgehog-interacting protein; *Hip*; *Hhip*), a transmembrane protein that attenuates signalling (Chuang and McMahon, 1999), and *Boc* (biregional Cdon-binding protein), a Robo-related Shh-binding protein (Tenzen et al., 2006). Although expression of some of these components has been reported in the mouse retina (Wallace and Raff, 1999; Wang et al., 2005), it is not clear whether they are distributed differently among the I- and C-RGCs.

Zic2-positive I-RGCs are generated at E14.5 in the ventrotemporal (VT) crescent of the retina (Herrera et al., 2003). *Isl2*-positive C-RGCs instead occupy the entire retina (Pak et al., 2004). Double labelling with GFP and *Zic2* antibodies of E14.5 retinal sections from *Shh::GFP^{Cre/+}* embryos, in which GFP expression mimics endogenous *Shh* mRNA distribution (Harfe et al., 2004), showed that the entire population of differentiated C-RGCs expresses *Shh*, in agreement with *Shh* mRNA distribution, whereas the vast majority of I-RGCs do not (Fig. 1A,C-E). This difference was still observed at E16.5 (not shown), indicating that a lack of *Shh* expression does not imply ongoing I-RGC differentiation. Conversely, *Boc*, which together with *Smo* mediates *Shh* chemoattraction on precrossing commissural axons (Okada et al., 2006), was expressed in the I-RGCs but not in the C-RGCs (Fig. 1G,I). Low *Boc* expression was also detected in the remaining retinal neuroepithelium. Similarly, *Ptc2* mRNA was detected in a subpopulation of RGCs in the VT crescent and in neuroblasts dispersed throughout the retinal neuroepithelium (Fig. 1F,H). In contrast to this differential distribution, *Ptc1* and *Hip1*, which seems to participate in the Shh-mediated chemorepulsion on postcrossing commissural axons (Bourikas et al., 2005), were homogeneously distributed in all RGCs and in the remainder of the retinal neuroepithelium (Fig. 1B,J). *Gli1-3* expression was either restricted to the neuroblast layer (*Gli1*; not shown) or homogeneously expressed in all RGCs (*Gli2*, Fig. 1K; *Gli3*, not shown).

Shh inhibits neurite outgrowth from C-RGCs but promotes that from I-RGCs

The differential expression of *Shh* receptors in the mouse I- and C-RGCs and their different trajectory at the chiasm midline suggested that their axons might respond differently to *Shh* exposure. To test

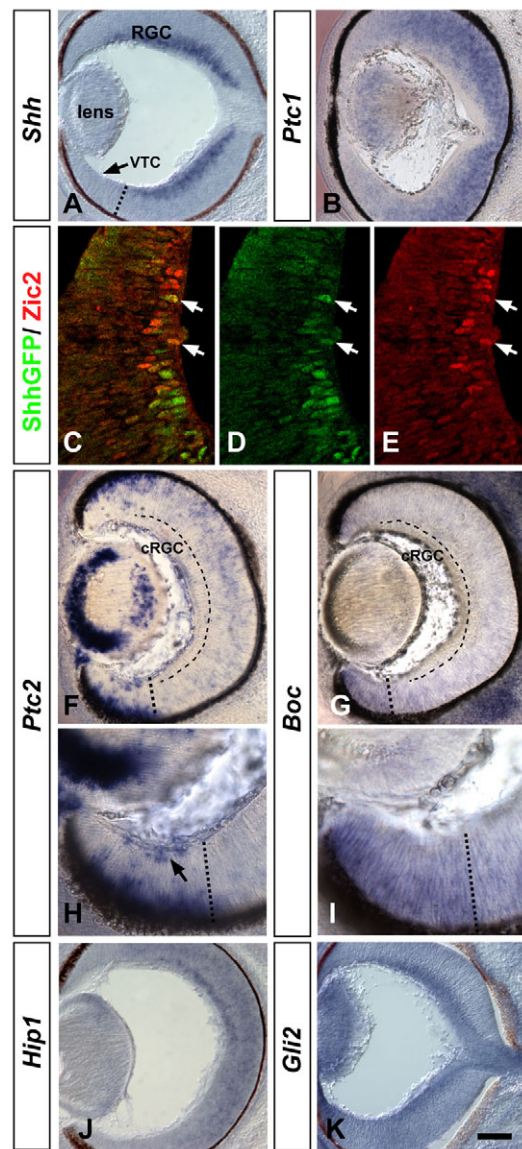


Fig. 1. Components of the Shh signalling pathway are differentially expressed in I-RGCs and C-RGCs. (A,B,F-K) In situ hybridisation analysis of coronal sections from E14.5 mouse embryos as indicated. (C-E) Similar sections from *Shh::GFP^{Cre/+}* E14.5 embryos double labelled for GFP (green) and *Zic2* (red); overlay in yellow. *Shh* mRNA localises to most of the RGC layer but is absent from the ventrotemporal crescent (VTC), where only rare *Zic2*/GFP⁺ cells are observed (arrows in A,C-E). *Ptc2* (F,H) and *Boc* (G,I) are expressed in the VTC (thick dotted line) but not in C-RGCs (thin dashed line). *Ptc1* (B) and *Hip1* (J) are distributed throughout the neuroepithelium and *Gli2* (K) localises to the RGC layer. cRGC, contralateral projecting RGCs. Scale bar: 200 μ m in A,B,F,G,J,K; 30 μ m in C-E; 35 μ m in H,I.

this, explants from E14.5 VT (I-RGC) and dorsonasal (DN) (a C-RGC source) retinas were grown on laminin for 24 hours in the presence or absence of *Shh* (1 μ g/ml). Under control conditions, VT and DN explants extended numerous neurites that occupied similar areas of outgrowth (Fig. 2). Upon *Shh* addition, VT explants significantly increased their growth area, whereas DN explants did not (Fig. 2). Similar results were obtained when retinal explants were grown in collagen gels for 48 hours (see Fig. S1A in the supplementary material).

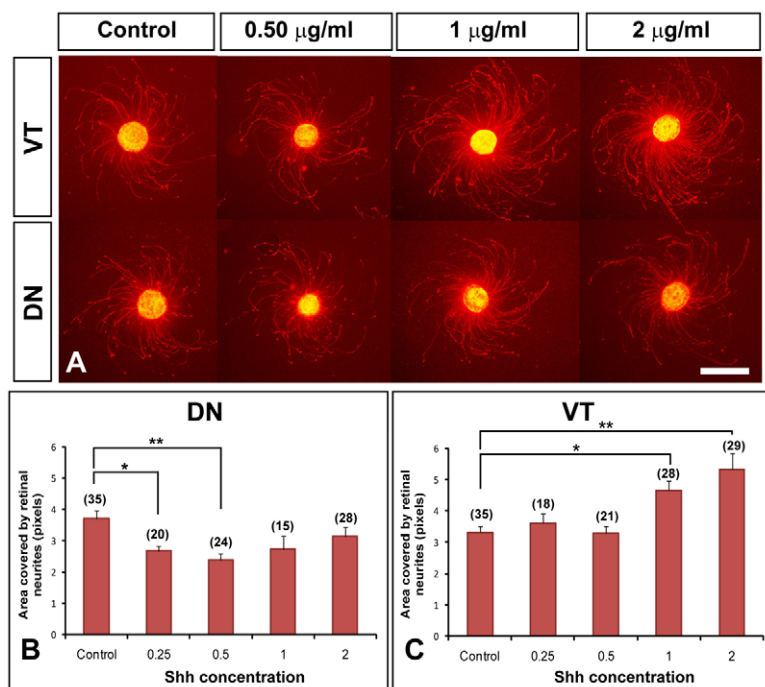


Fig. 2. Shh promotes neurite outgrowth from VT explants but inhibits neurite outgrowth from DN explants. (A) Ventrotemporal (VT) and dorsonasal (DN) explants grown in the presence of different Shh concentrations. Outgrowth was visualised by staining with phalloidin. (B,C) Quantification of neurite outgrowth from DN (B) and VT (C) explants. Bar graphs show the area covered by neurites (in pixels). The number of explants analysed is indicated above each bar. * $P < 0.05$, ** $P < 0.01$ (one-way ANOVA). Scale bar: 500 μm .

Shh activity on chick retinal axons may depend on protein concentration (Kolpak et al., 2005). Our data could therefore reflect a differential sensitivity of the VT and DN retinal explants to Shh concentration. To test this, VT and DN explants were exposed to a range of Shh doses (0.25–6 $\mu\text{g/ml}$). Notably, the extent of outgrowth from VT explants was significantly increased at high concentrations (Fig. 2A,C), whereas that from DN explants was reduced at low Shh concentrations (Fig. 2A,B), indicating a differential activity of Shh on I- versus C-RGCs. These differences were not due to changes in RGC differentiation because Shh treatment did not modify the levels of *Zic2* and *Isl2* (real-time PCR, not shown).

Shh does not reorient chick visual fibre growth, but rather induces growth cone arrest and retraction (Trousse et al., 2001). If mouse C-RGC neurites behave as chick RGC axons, a similar behaviour should be expected in the presence of a focal source of Shh. Indeed, Shh-soaked beads (1 $\mu\text{g}/\mu\text{l}$) placed at $\sim 100 \mu\text{m}$ from the DN explants did not deflect the growth of the fibres (not shown), but considerably reduced neurite length as compared with controls (see Fig. S1B in the supplementary material). This effect was reversed by the addition of cyclopamine, a Smo activity inhibitor (Frank-Kamenetsky et al., 2002). Similarly, the direction of outgrowth from VT explants was not modified by the presence of Shh-soaked beads but, in contrast to DN explants, the length of their neurites was not affected (see Fig. S1B in the supplementary material), possibly owing to an insufficient local concentration of the morphogen.

Blockade of Shh alters the distribution of RGC axons at the optic chiasm

We have previously hypothesised that Shh present at the chiasm borders might serve to anteroposteriorly restrict the midline growth of contralateral projecting axons (Trousse et al., 2001). If Shh plays a similar function in mice, we would expect that neutralising Shh activity would scatter contralateral projections at the optic chiasm without interfering with I-RGC fibres, which never cross the SSEA-1-positive midline cells (Mason and Sretavan, 1997), thus causing them to turn into the ipsilateral optic tract at a distance from the Shh source (Fig. 3E).

To test this prediction, we injected hybridoma cells producing anti-Shh blocking antibodies directly into the amniotic sac of mouse embryos, a proven method to interfere with endogenous Shh activity (Merchan et al., 2007). Embryos were injected at E13.5, when retinal fibres just approach the optic chiasm (Bovolenta and Mason, 1987), and analysed at E18.5, when the majority of fibres should have reached their targets. Complete unilateral DiI-filling of the optic nerve head of uninjected embryos ($n=6$) or control hybridoma-injected embryos ($n=7$) revealed a normal trajectory: retinal axons extended toward the midline, where the majority crossed and entered the contralateral optic tract, while only a small proportion projected into the ipsilateral tract (Fig. 3A,C,E). A few fibres were observed extending into the contralateral optic nerve, as reported previously (Plump et al., 2002). Notably, significant differences were observed in anti-Shh-injected embryos ($n=11$): the overall region occupied by DiI-labelled fibres at the midline was enlarged, fibres appeared less fasciculated and many wandered, extending in an aberrant posterior direction (Fig. 3B,E). Indeed, there was a 30% increase in the midline scattering of the fibres in anti-Shh-treated embryos compared with untreated or control-treated embryos, as determined by measuring the region occupied by DiI-labelled axons at the level of the chiasm (Fig. 3D). Thus, Shh activity is normally needed to constrain and fasciculate the growth of contralateral projecting visual fibres at the chiasm.

Furthermore, the number of axons that invaded the contralateral optic nerve and that grew ipsilaterally was significantly increased (Fig. 3B,E). Owing to the considerable number of axons that projected ectopically, it was difficult to quantify the precise number of fibres that took one of the abnormal trajectories in these preparations. To assess the origin of the fibres that invaded the ipsilateral optic tract and thereby determine possible alterations in the behaviour of I-RGC axons, we performed retrograde unilateral labelling from the optic tract and analysed the distribution of DiI-labelled fibres in both the ipsilateral and contralateral retinas. If the growth of I-RGC axons was affected by anti-Shh treatment (slower growth or misprojections) then a differential labelling in the VT quadrant of the ipsilateral retina was expected. However, no differences were observed in this quadrant

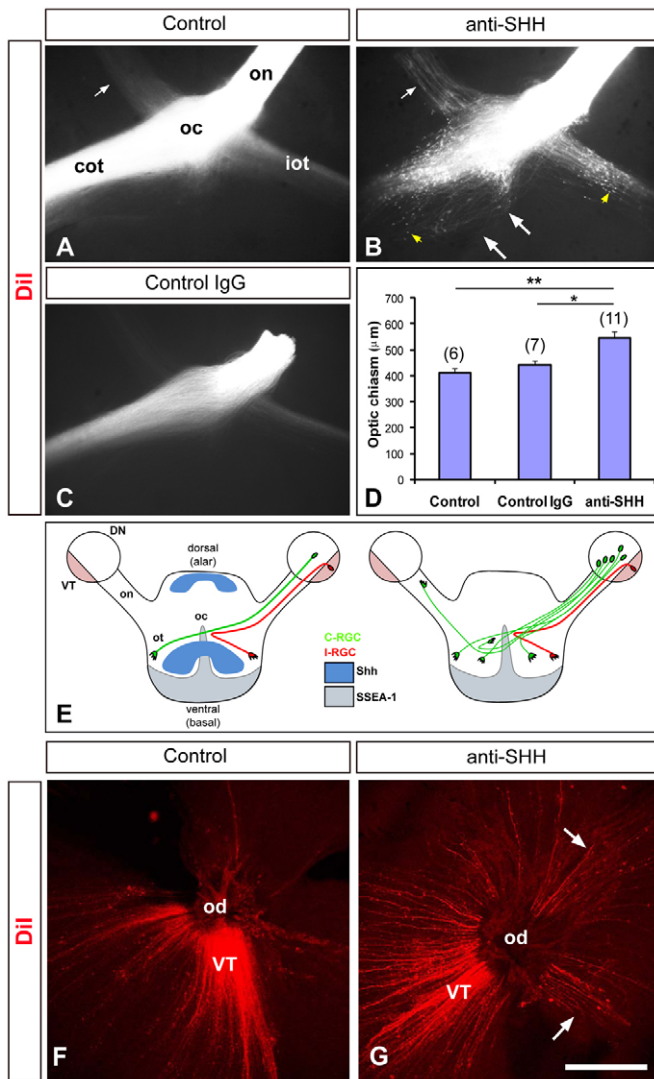


Fig. 3. Shh neutralisation alters the distribution of RGC axons at the optic chiasm. (A–C) Ventral views of the proximal visual pathway from E18.5 non-injected (A) and from anti-Shh (B) and control IgG (C) hybridoma-treated mouse embryos visualised by complete Dil filling. Anterior is to the top. In anti-Shh-treated embryos, axons spread at the chiasm (large white arrows in B), and ipsilateral tract and contralateral nerve (small white arrow, compare with A) projections appear increased; growth cones accumulate along the path (yellow arrows). (D) Quantification of the width occupied by Dil-labelled fibres at the chiasm in untreated ($n=6$), control-treated ($n=7$) and anti-Shh-treated ($n=11$) embryos ($*P<0.05$, $**P<0.01$, one-way ANOVA). (E) Schematic ventral view of the proximal visual system depicting fibre trajectory and Shh and SSEA-1 distribution in control (left) and anti-Shh-treated (right) embryos. (F,G) Confocal images of flat-mounted E18.5 ipsilateral retinas showing Dil retrograde labelling from the optic tract in control and anti-Shh-treated embryos. Arrows in G indicate the presence of abnormal retrograde labelling in quadrants other than VT. cot, contralateral optic tract; iot, ipsilateral optic tract; oc, optic chiasm; od, optic disc; on, optic nerve; ot, optic tract. Scale bar: 500 μm in A–C; 215 μm in F,G.

when control ($n=4$) and treated ($n=7$) ipsilateral retinas were compared (Fig. 3F,G and see Fig. S2G,H in the supplementary material). By contrast, an abnormal number of backfilled fibres was present, particularly in the DT quadrant of the ipsilateral retina (Fig. 3G and

see Fig. S2G,H in the supplementary material), indicating that a number of axons deriving from C-RGCs were aberrantly projecting to the ipsilateral optic tract in anti-Shh-treated embryos. Together, these data explain the apparent increase in the number of ipsilateral projecting fibres observed with anterograde labelling and suggest that interference with Shh mostly affects the behaviour of C-RGC axons at the midline.

A tight regulation of Shh activity is required to pattern the ventral forebrain (Placzek and Briscoe, 2005). However, at E13.5, when the hybridomas were injected, Shh activity should no longer be required in the preoptic-hypothalamic region (Manning et al., 2006). Accordingly, treatment with Shh-neutralising antibodies did not perturb the morphology of the chiasm as shown by immunostaining of midline glial and neuronal cells with Gfap and SSEA-1 antibodies (see Fig. S2C–F in the supplementary material), supporting a direct link between the interference with Shh activity and the observed alterations in the RGC axon trajectory.

Alterations in the levels of Shh signalling cause transcription-dependent changes in RGC growth cone morphology

In addition to the defects described above, we observed an abnormally frequent number of growth cones accumulating in the chiasm and both optic tracts (Fig. 3B; see Fig. S2A,B in the supplementary material). Furthermore, fewer fibres appeared to reach the optic tract in the anti-Shh-treated embryos than in the controls (Fig. 3A–C), suggesting slower growth of the fibres. Because C-RGCs express Shh (Fig. 1A), this source of morphogen could contribute to the advance of the growth cones even before they reach the midline. If this were the case, Shh should be transported and released by the RGC growth cones, as previously suggested (Wallace and Raff, 1999; Traiffort et al., 2001). Accordingly, floor plate cells (a positive control) as well as axons and growth cones from DN explants, but not those from VT and dorsal root ganglia (a negative control) explants, showed a clear accumulation of Shh immunolabelling (Fig. 4A,B; see Fig. S3 in the supplementary material). Furthermore, if RGC-derived Shh contributes to the movement of growth cones, neutralisation of Shh activity should modify their morphology. To test this, we used the growth cone collapse assay, which uses growth cone morphology as a readout of the treatment activity (Kapfhammer and Raper, 1987). VT and DN explants were cultured on laminin for 24 hours and then treated with different reagents for 30 minutes, fixed and analysed. Under these conditions, the majority of untreated retinal growth cones exhibited a widespread morphology, whereas 24.7% (in VT, $n=409$) to 31.5% (in DN, $n=426$) presented a ‘collapsed’ morphology (see Materials and methods for definition) (Fig. 4C). Incubation with cyclopamine alone significantly increased the number of collapsed growth cones (VT, $n=121$; DN, $n=110$) compared with vehicle-treated explants (not shown). This effect was evident in both DN and VT explants, whereas Shh neutralisation with antibodies was effective only in VT explants (Fig. 4D,E), possibly reflecting a more efficient neutralisation in VT explants, in which the endogenous levels are expected to be lower owing to the coexistence of Shh-negative (I-) and Shh-positive (C-) RGCs. Conversely, treatment of the growth cones with exogenous Shh (VT, $n=146$; DN, $n=163$) or with the Smo agonist SAG (VT, $n=208$; DN, $n=135$) decreased the number of growth cones with collapsed morphology, although this effect was more evident in the growth cones from DN explants (Fig. 4D,E).

Activation of the Shh signalling cascade ultimately leads to gene transcription. However, it is unclear whether Shh activity on growth cones requires this nuclear event or whether it might simply rely on

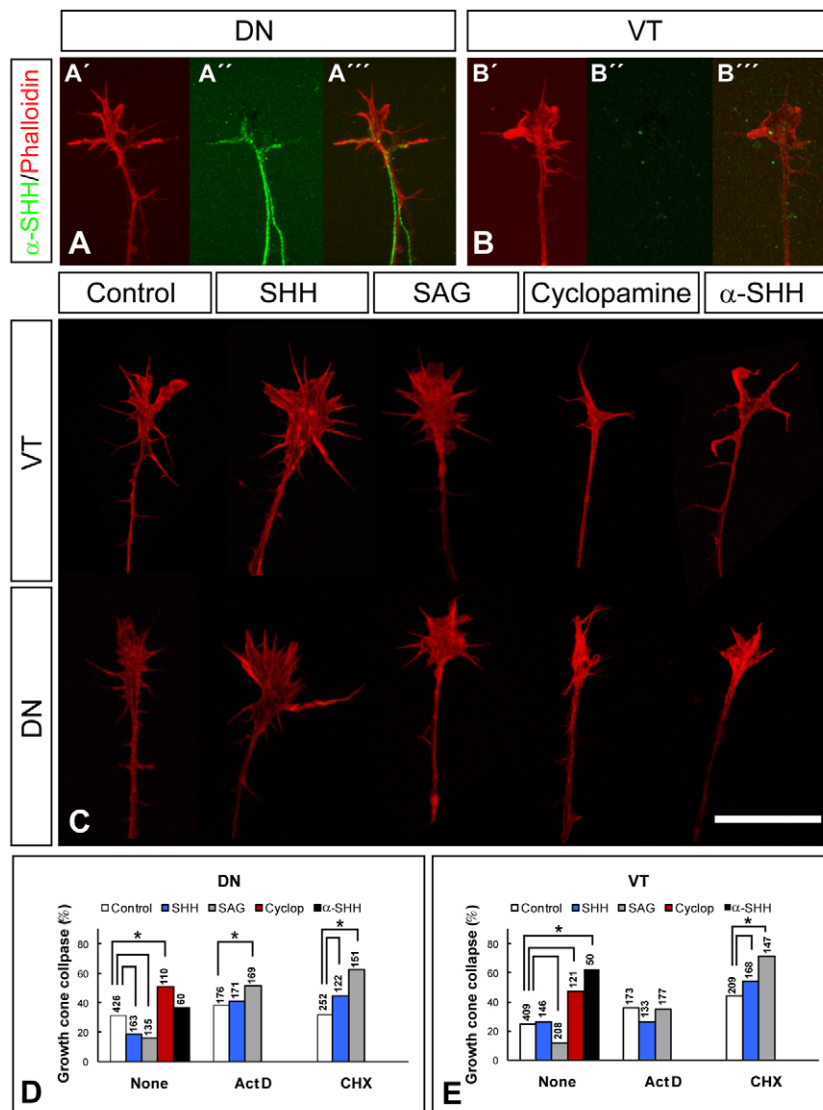


Fig. 4. Modulation of RGC-derived Shh signalling causes transcriptional-dependent changes in growth cone morphology.

(A, B) Axons and growth cones from DN (A) and VT (B) explants immunostained with antibodies against Shh (green) and counterstained with phalloidin (red). Individual channels in A', A'', B', B'' with overlays in A''', B'''. (C) Confocal images of VT (I-RGC) and DN (C-RGC) growth cones exposed for 30 minutes to PBS (control), Shh, SAG, cyclopamine or anti-Shh antibody. (D, E) Percentage of collapsed growth cones in DN and VT explants after activation or inhibition of Shh signalling in the presence or absence of actinomycin D (ActD) or cycloheximide (CHX). The number of growth cones analysed is indicated above each bar. ActD and CHX prevent the decrease in growth cone collapse induced by Shh or SAG. * $P < 0.05$ (contingency table with Fisher's exact test). Scale bar: 25 μm in A, B; 20 μm in C.

local changes in secondary messengers, such as cAMP, the growth cone levels of which are modified upon Shh exposure (Trousse et al., 2001). To address this, we tested whether the addition of actinomycin D, a transcription inhibitor, modified the response to Shh signalling activation in the collapse assay. In both DN and VT explants the addition of actinomycin D alone, 10 minutes prior to ligand addition, slightly increased the number of collapsed growth cones (by ~10%) as compared with untreated explants. Addition of SAG increased whereas exogenous Shh did not significantly modify this level of collapse, implying that the presence of actinomycin D abrogated the ability of Shh/SAG to reduce growth cone collapse (Fig. 4D, E). Addition of cycloheximide, a translation inhibitor, had similar or stronger effects (Fig. 4D, E), a possible reflection of protein synthesis being locally active in response to a number of guidance cues (VanHorck and Holt, 2008).

Interference with RGC Shh signal transduction causes axonal navigation defects in the proximal visual pathway

In vivo blockade of Shh as well as interference with endogenous activity in retinal explants suggested that RGC-derived Shh might contribute to control growth cone movement cell-autonomously. To

further corroborate this idea, we used in utero electroporation to transflect RGCs with a Shh-insensitive version of patched, $Ptc1^{\Delta loop2}$, which dominantly represses Shh signal transduction (Briscoe et al., 2001). If RGC-derived Shh is cell-autonomously required to direct axon extension, abrogation of signal transduction should cause defects in RGC axon outgrowth before growth cones reach the chiasm.

$pCAGGS-Ptc1^{\Delta loop2}-IRES-GFPnls$ together with $pCAGGS-EGFP$ ($n=8$) or $pCAGGS-EGFP$ alone ($n=5$) were electroporated in the eye of E13.5 embryos, which were then analysed at E16.5. In all embryos, EGFP-positive transfected cells occupied the central portion of the retina and corresponded to $Isl2^+$ C-RGCs (Fig. 5C), whereas $Zic2^+$ I-RGCs never showed EGFP expression (Fig. 5A, B), indicating that their capacity to sense Shh was not affected. In the $Ptc1^{\Delta loop2}-EGFP$ electroporated tissue, the endogenous mRNA levels of $Ptc1$, $Ptc2$ and $Hip1$, which are transcriptional targets of Shh signalling (Chuang and McMahon, 1999; Goodrich et al., 1996; Pearse et al., 2001), were decreased compared with controls, indicating that the transgene effectively blocked signal transduction in the retina (Fig. 5D).

Normally, RGC axons grow in the fibre layer with a radially oriented, organised pattern that converges at the optic disc, where a specialised group of $Pax2^+$ glial cells provide guidance

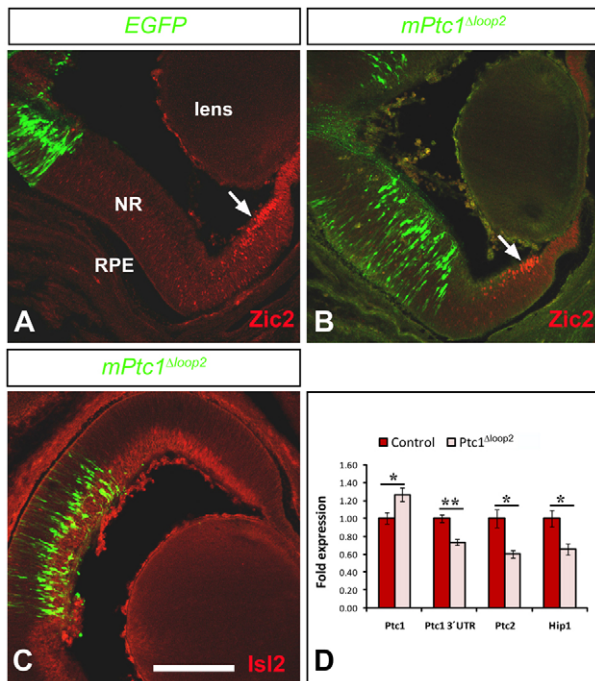


Fig. 5. Electroporation of *Ptc1*^{Δloop2} effectively blocks Shh signal transduction in the central retina. (A–C) Coronal sections of E16.5 retinas electroporated with *EGFP* and *Ptc1*^{Δloop2} (B,C) or *EGFP* alone (A) and immunostained with anti-Isl2 (C-RGCs) or anti-Zic2 (I-RGCs, arrows). (D) Quantitative RT-PCR analysis of *Ptc1*, *Ptc2* and *Hip1* mRNA levels. Values were normalised to 18S rRNA. In *Ptc1*^{Δloop2}-electroporated retinas, the endogenous levels of *Ptc1* (*Ptc1* 3'UTR), *Ptc2* and *Hip1* mRNA are significantly reduced. Primers recognising the *Ptc1*^{Δloop2} form (*Ptc1*) confirmed effective plasmid transduction. Values represent the mean ± s.e.m. of two independent experiments performed in triplicate. **P*<0.05, ***P*<0.01 (Student's unpaired *t*-test). Scale bar: 200 μm.

information to the axons (Dakubo et al., 2003; de la Torre et al., 1997; Morcillo et al., 2006). This pattern was clearly visible in flat-mount or frontal sections of *EGFP*-control retinas at E16.5 (Fig. 6A,B,D,E), when most of the growth cones from the transfected RGCs have long passed through the disc. In *Ptc1*^{Δloop2}-transfected retinas, the centripetal orientation of the axons at the optic disc was lost despite a normal organisation of the Pax2⁺ glial cells (Fig. 6F). In all the *Ptc1*^{Δloop2} embryos analysed, many *EGFP*-positive axons wandered, either growing parallel to the disc (Fig. 6C,F) or away from it, invading the peripheral retina (Fig. 6G–I). Several growth cones were still visible within the optic disc area (Fig. 6C), suggesting slower growth of the fibres. Similar alterations were observed in *EGFP*-electroporated fibres when Shh activity was neutralised by the injection of 5E1 (anti-Shh) hybridomas (see Fig. S4 in the supplementary material).

Defects were not limited to the eye cup. In three of the *Ptc1*^{Δloop2} embryos analysed, a few fibres turned sharply in the mid-optic nerve to grow dorsally, a route never observed in control embryos (Fig. 7A–C). In spite of these alterations, the axons of a large number of the *Ptc1*^{Δloop2}-*EGFP* transfected RGCs reached the chiasm area. Here, a number of axons turned into the ipsilateral side of the brain

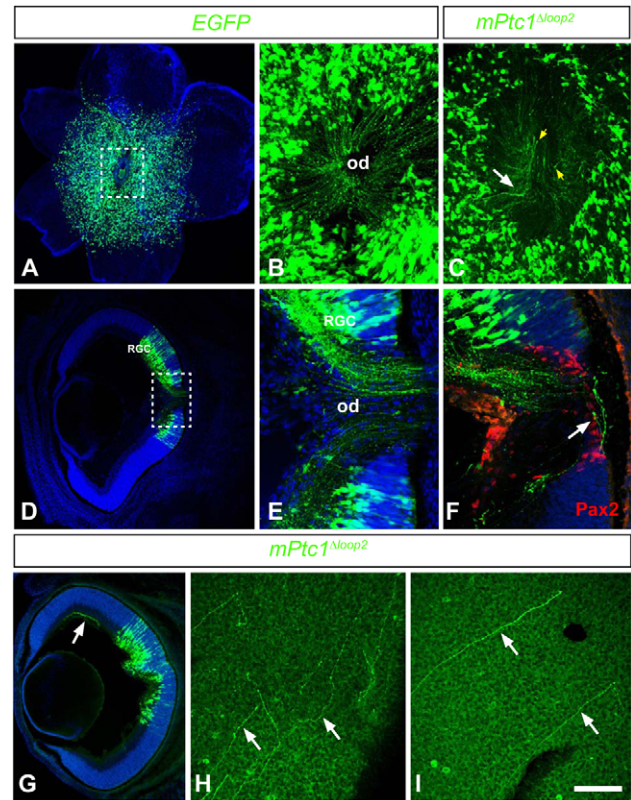


Fig. 6. Repression of Shh signal transduction in C-RGCs causes intraretinal guidance defects. Confocal images of flat-mounted (A–C,H,I) and horizontal sections (D–G) from E16.5 mouse retinas electroporated with *EGFP* or *EGFP-Ptc1*^{Δloop2}. Immunolabelling for Pax2 is in red (F). In *Ptc1*^{Δloop2}-positive retinas, radial organisation is lost (C,F), fibres turn in aberrant directions including towards the periphery (arrows in C,F,G–I). Growth cones (yellow arrows, C) accumulate in the optic disc (od). The boxed regions in A and D indicate the locations of the high-magnification images shown in B and E, respectively. Scale bar: 200 μm in A,D,G; 75 μm in B,C,H,I; 100 μm in E,F.

(Fig. 7D), although the electroporations hit only the Isl2⁺ C-RGCs. The remaining fibres reached the midline, but wriggled or turned back in a disorganised growth pattern (Fig. 7E,F).

Together, these observations strongly support the notion that transduction of Shh signalling is continuously required along the proximal visual pathway to foster and direct axon growth (Fig. 7G,H).

DISCUSSION

An increasing body of evidence highlights a direct and prominent role for Shh signalling in the control of motility of multiple cell types during embryonic development. *Drosophila* germ and tracheal cells, vertebrate fibroblasts, angioblasts, neural crest cells, oligodendrocyte precursors and growth cones of RGCs and spinal cord commissural neurons are among the targets of this Shh activity (Sanchez-Camacho et al., 2005; Deshpande et al., 2001; Gering and Patient, 2005; Kato et al., 2004; Kolpak et al., 2005; Merchan et al., 2007; Testaz et al., 2001; Vokes et al., 2004). In most of these examples, cells respond to Shh secreted by an adjacent signalling tissue. Here, we provide evidence that, in addition to this mechanism, proper navigation of mammalian C-RGC growth cones in the proximal visual pathway depends on Shh that is endogenously

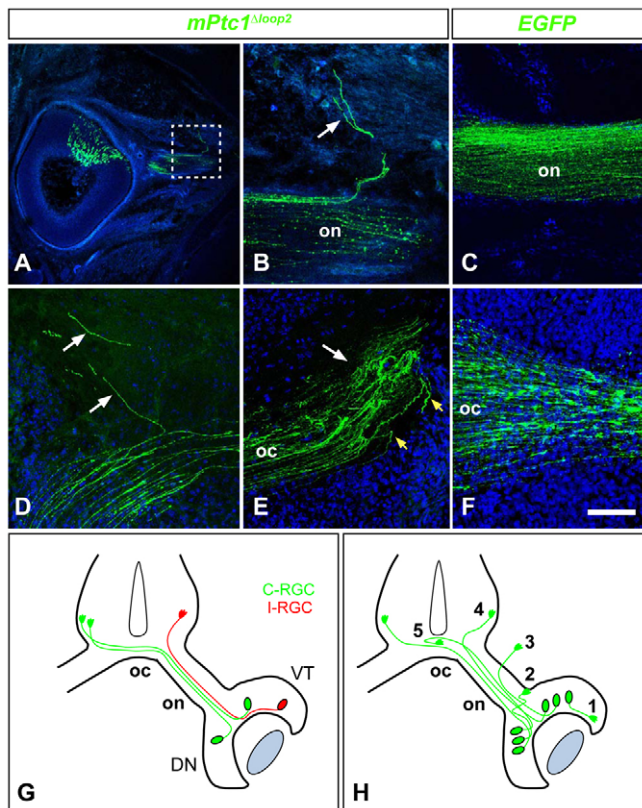


Fig. 7. Additional defects caused by the repression of Shh signal transduction in C-RGCs. Confocal images of the optic nerve (A–C) or chiasm (D–F) from EGFP (C, F) or EGFP/Ptc1 Δ loop2 (A, B, D, E) transfected mouse embryos at E16.5. In EGFP/Ptc1 Δ loop2-positive embryos, a few fibres leave the nerve (A, B, arrow), project to the ipsilateral optic pathway (D, arrows), form tangles (E, white arrow) or turn back (E, yellow arrows). The boxed region in A indicates the location of the high-magnification image shown in B. (G, H) Schematic view of the behaviour of visual axons in control (G) and EGFP/Ptc1 Δ loop2-transduced (H) C-RGCs. C-RGC axons are in green, I-RGC axons in red. Blockade of Shh signal transduction causes aberrant intraretinal growth (1, 2), abnormal optic nerve (3) or chiasm/tract (4, 5) turnings of C-RGCs axons. oc, optic chiasm; on, optic nerve. Scale bar: 200 μ m in A; 155 μ m in B–F.

produced by the C-RGCs themselves, highlighting a novel aspect of Shh-mediated motility control. We also show that, in contrast to C-RGCs, I-RGCs do not express Shh and, at least in vitro, respond differently to this morphogen. Because this behaviour correlates with the specific expression of *Boc* and *Ptc2* in I- but not C-RGCs, we hypothesise that differential activation of Shh signalling components might contribute to the divergence of I- from C-RGCs in the embryonic mouse retina.

C-RGC axon growth depends on two Shh sources: the RGC and the ventral midline

The expression of Shh together with other regulatory genes defines a domain in the developing hypothalamus that is important for determining the behaviour of retinal axons at the chiasm midline (Marcus et al., 1999). Downregulation of Shh expression in the optic recess area coincides with the arrival of pioneer RGC axons at the chiasm midline (Trousse et al., 2001). Conversely, abnormally expanded expression of Shh in this region

correlates with aberrant retinal axon growth (Macdonald et al., 1995; Torres et al., 1996; Trousse et al., 2001). Shh represses the growth of chick RGC axons in vitro and induces growth cone collapse (Trousse et al., 2001).

Confirming and extending these studies, we show here that neutralisation of Shh function causes abnormal growth of mouse C-RGC axons at the ventral forebrain. Defasciculation, aberrant projection to the contralateral optic nerve and ectopic caudal extension of visual fibres at the midline are the most prominent abnormalities, providing strong evidence that Shh present at the chiasm borders constrains retinal fibre growth to the contralateral side of the brain, as we previously hypothesised (Trousse et al., 2001).

In zebrafish mutants in which components of the Hh signalling pathway are affected, RGC axons fail to cross the midline (Culverwell and Karlstrom, 2002). Detailed analysis of these mutants and the treatment of wild-type zebrafish embryos with cyclopamine demonstrated that axon guidance defects were secondary to the Shh-mediated specification of midline glial cells as well as to the control of Slit expression (Barresi et al., 2005; Culverwell and Karlstrom, 2002), a potent repellent for RGC axons (Erskine et al., 2000; Niclou et al., 2000; Ringstedt et al., 2000). Although in our experiments anti-Shh-producing cells were injected when Shh expression is already downregulated and no longer needed in the preoptic area (Manning et al., 2006; Trousse et al., 2001), we cannot entirely exclude the possibility that some of the observed defects might be secondary to subtle patterning alterations. However, we strongly favour a direct effect of midline-derived Shh on mouse visual fibre growth, for a number of reasons. Shh addition changes growth cone morphology in short-term in vitro assays causing net differences in the overall outgrowth after 24 or 48 hours. In anti-Shh-treated embryos, cells positive for Gfap and SSEA-1, which are necessary for visual fibre sorting at the chiasm (Mason and Sretavan, 1997), are formed normally. In addition, *Slit1*- or *Slit2*-null mice have no apparent visual phenotype, whereas double-knockout mice are characterised by an additional anteriorly positioned ectopic chiasm (Plump et al., 2002), a phenotype clearly different from that observed in the anti-Shh-treated embryos. Similarly, the genetic inactivation or perturbation of a number of other molecules known to influence midline crossing or sorting of visual fibres, including ephrin B2, CD44 and Nrcam (Lin and Chan, 2003; Nakagawa et al., 2000; Williams et al., 2006; Williams et al., 2003), causes defects that do not mimic those observed in the anti-Shh-treated embryos. This argues that Shh inactivation does not act by altering the expression of these factors, although we cannot formally rule out the possibility that Shh signalling might be needed to maintain the expression of other, as yet unidentified molecules. Alterations similar to those observed in anti-Shh-treated embryos, including abnormal turning in the contralateral optic nerve, were observed upon genetic or enzymatic elimination or modification of proteoglycan sugar moieties (Chung et al., 2000; Inatani et al., 2003; Pratt et al., 2006), which are important for Shh diffusion (Guerrero and Chiang, 2007), supporting a direct relationship between Shh activity and axon growth. Furthermore, interference with Shh activity in brain slices appears to cause visual axon routing abnormalities similar to those we observed in vivo (Hao et al., 2006).

Consistent with the presence of additional inhibitory cues responsible for channelling retinal axon growth across the chiasm, the defects observed in anti-Shh-treated embryos were not extensive. Thus, the rostral expression of Slit2 (Erskine et al., 2000) may

restrain retinal axons from entering the preoptic area in the absence of Shh activity, whereas Slit1 together with other components expressed by SSEA-1-positive cells (Marcus and Mason, 1995) may partially counterbalance the loss of Shh activity, limiting the number of axons that abnormally invade the hypothalamic area in anti-Shh-treated embryos (Fig. 3E).

In addition to defasciculation at the chiasm, anti-Shh antibodies caused an abnormal accumulation of growth cones along the proximal visual pathway, suggesting that Shh might also modulate axon extension. Because it is unlikely that midline-derived Shh can diffuse as far as the optic nerves, we hypothesised that Shh produced by the RGCs themselves could be responsible for this effect. Indeed, Shh is transported along the axons as previously suggested (Traiffort et al., 2001; Wallace and Raff, 1999) and is strongly present in the C-RGC growth cones. Modifications to growth cone behaviour observed after the addition of cyclopamine to retinal explants, as well as axon misprojections in the proximal visual pathway after inhibition of Shh transduction in C-RGCs, confirmed that Shh influences axon growth by a cell-autonomous mechanism (Shh produced by the population of RGCs and acting over the population itself). This is particularly intriguing because there are only a few examples of such a mechanism in axon guidance. The activity of Bdnf on pyramidal dendritogenesis (Wirth et al., 2003) and that of ephrin A on RGCs represent such cases (Hornberger et al., 1999).

Owing to the size of the eye and the lack of transparency of the uterus, it was very difficult to successfully perform targeted electroporation before E13.5. Given that the transgene may need several hours to reach full expression, inhibition of Shh transduction in the targeted cells should be effective only from E14–14.5. By that time, many of the axons of the electroporated C-RGCs have reached or passed the chiasm, which explains why several GFP-positive axons in the *Ptc1^{Δloop2}* embryos showed a normal initial trajectory. The misprojection of a significant number of fibres at different points along the proximal trajectory is instead likely to reflect the position reached by the individual growth cones when their ability to sense the presence of Shh was abolished, underscoring a continuous effect of Shh on fibre extension along the entire proximal visual pathway.

Cell-autonomous (RGC-derived) Shh appeared to have a positive effect on C-RGC axon growth, whereas the effect of the non-cell-autonomous (midline-derived) Shh appeared to be negative. This discrepancy can be easily reconciled in the following model. From their initial extension, C-RGC axons grow in the presence of a low-level Shh gradient created by secretion from the axons themselves as they progress along the proximal path. Because the cellular response to Hh gradients is determined by the ratio of occupied to unoccupied Ptc receptor (Casali and Struhl, 2004), low occupancy may lead to a positive effect in the growth cone, maintaining cytoskeletal organisation and possibly also transcriptionally regulated levels of guidance cue receptors. Continuous Shh presence along the nerve could lead to adaptation, an important mechanism that controls the response of growth cones to guidance cues (Ming et al., 2002; Piper et al., 2005; Rosentreter et al., 1998). Adaptation changes the threshold of ligand concentration needed to induce a response (Piper et al., 2005) such that a critical concentration might then be required to obtain a response (Rosentreter et al., 1998). This abrupt change in Shh concentration must occur at the chiasm region where an additional Shh source is present. Thus, a sharp change in the number of occupied receptors causes a different and negative response of the C-RGC growth cones to Shh, funnelling axon growth to the contralateral side of the brain.

Differential effects of Shh on I-RGC versus C-RGC axons

The above model explains the behaviour of the C-RGC axons as observed in the different experimental paradigms employed in this study. However, whether it applies to I-RGCs is unclear. Technical limitations prevented electroporation of the *Ptc1^{Δloop2}* construct in the VT crescent of the retina, so we could not clearly establish the *in vivo* behaviour of I-RGCs following interference with Shh signalling. Although retrograde labelling experiments suggest that midline-derived Shh mostly affects C-RGC axons, we cannot exclude the possibility that the difference observed *in vitro* between I- and C-RGC axons might reflect an effect that Shh secreted by C-RGCs may exert on I-RGCs as they grow in the initial portion of the visual trajectory. Thus, in contrast to C-RGCs, high concentrations of Shh consistently promoted I-RGC axon outgrowth and the spreading of their growth cones. Notably, this response correlates with the specific expression of the Shh receptors *Boc* and *Ptc2* in I- but not C-RGCs. Although the functions of *Ptc2* have hardly been studied (Pearse et al., 2001), *Boc* activity has recently been associated with the Shh-induced attraction of commissural axons (Okada et al., 2006), which interestingly show a dual response to Shh depending on the activated receptor: *Smo* and *Boc* mediate chemoattraction of precrossing commissural axons (Charron et al., 2003; Okada et al., 2006), whereas *Hip1* seems to be involved in repulsion of postcrossing axons (Bourikas et al., 2005). The growth-promoting effect of Shh on I-RGCs might involve a similar *Boc* activation.

An additional interesting difference is that most I-RGCs do not express Shh. It is unclear what impact this might have on axon extension, as I-RGC axons grow intermixed with C-RGC axons that release Shh. The difference is more likely to relate to cell specification. Diffusion of ventrally located Shh appears to control *Zic2* expression in the dorsal telencephalic midline (Hayhurst et al., 2008), suggesting that *Zic2* activation responds to a low level of the morphogen. In the retina, Shh diffusing from the adjacent C-RGCs might activate *Zic2* in I-RGCs, which in a feedback loop may repress Shh, given that *Zic2* mRNA is absent from the optic vesicles of *Shh*-null mice (Brown et al., 2003). This regulatory loop would reinforce the divergence of the two RGC cell types and their specific projections, as has been proposed for a possible *Isl2* and *Zic2* cross-repression (Butler and Tear, 2007; Pak et al., 2004).

Molecular mechanisms underlying Shh-mediated effects on growth cones

A general question relating to the axon guidance function of cell signalling pathways, including Shh, BMP and Wnt, is whether their activation leads simply to local changes in cytoskeletal components within the growth cones or whether it also involves the control of gene transcription (Bovolenta et al., 2006). At least for the Shh pathway, the two mechanisms are not mutually exclusive and are likely to coexist, although additional studies are needed to obtain a detailed picture of this. In the chick embryo, decreased intracellular levels of cAMP may underlie the effect of Shh on RGC growth cone movement (Trousse et al., 2001), whereas a novel transcription-independent mechanism involving arachidonic acid metabolism seems to mediate the Shh-induced migration of mesenchymal fibroblasts (Bijlsma et al., 2007). Here we have shown that incubation with actinomycin D or cycloheximide abrogates the Shh-induced spreading of the growth cone, indicating that transcription and translation are needed for these changes. Possible targets of these activities are proteins involved in actin organisation, such as *Lasp1* or *Mim* [missing in metastasis; also known as basal cell carcinoma-enriched gene 4 (*Beg4*)], which are regulated by Shh signalling in

other contexts (Gonzalez-Quevedo et al., 2005; Ingram et al., 2002). Nevertheless, it has yet to be established whether transcription/translation in response to Shh occurs only in the cell body or whether local protein synthesis, an important mechanism to control the growth cone response to guidance cues (VanHorck and Holt, 2008), is also needed.

In conclusion, we have shown that Shh signalling plays a prominent role in controlling axon extension along the proximal visual pathway and in funnelling C-RGC axons to the contralateral side of the brain. A cell-autonomous and a non-cell-autonomous mechanism, with apparently opposite effects, cooperate to achieve these functions. The key to the differential response may lie in a concentration gradient of ligand, thus providing a good example of true morphogenetic activity in axon guidance. Whether Shh signalling contributes to the functional differences between I- and C-RGC projections, as suggested by expression analyses and in vitro studies, awaits further confirmation in vivo.

We thank Dr C. A. Mason for helpful suggestions and critical reading of the manuscript; Drs E. Herrera and C. García-Frigola for sharing their expertise in electroporation in utero; C. Hernández-Capitán for assistance with confocal microscopy; L. Barrios (CTI, CSIC) for advice with the statistical analysis; and Drs J. K. Chen, S. Brown, E. Marti, S. L. Pfaff, S. Pons and M. Torres for kindly providing the following reagents: SAG agonist, anti-Zic2 antibody, the *Ptc1^{loop2}-IRES-GFPnls* construct, anti-Is12 antiserum, purified N-Shh and *Shh::GFPnls* embryos, respectively. This work was supported by grants from the Spanish MEC (BFU-2004-01585), Fundación la Caixa (BM04-77-0), Fundación Mutual Madrileña (2006-0916) and Comunidad Autónoma de Madrid (CAM, P-SAL-0190-2006) to P.B. C.S.-C. held a contract from the 'Juan de la Cierva' Program from the Spanish MEC and is now supported by the CSIC JAE program.

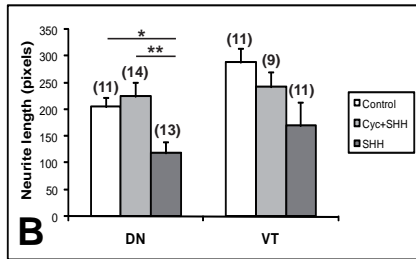
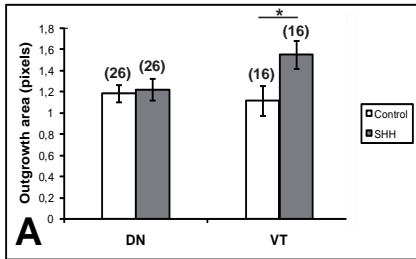
Supplementary material

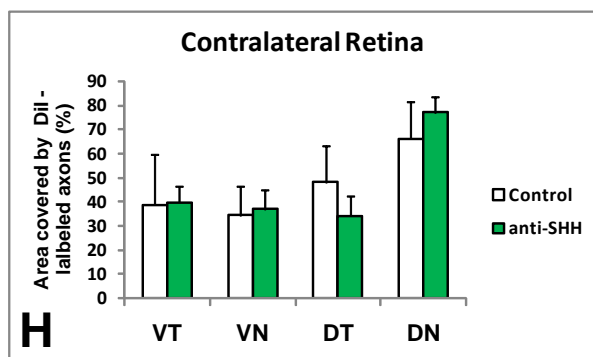
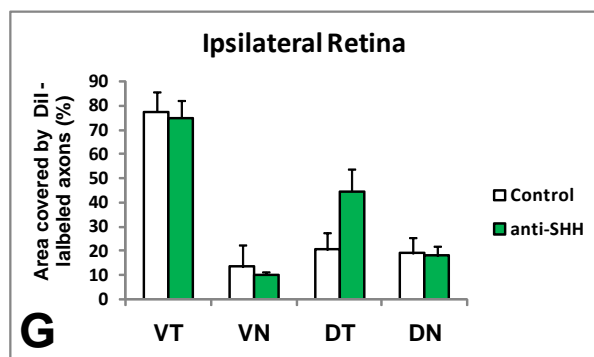
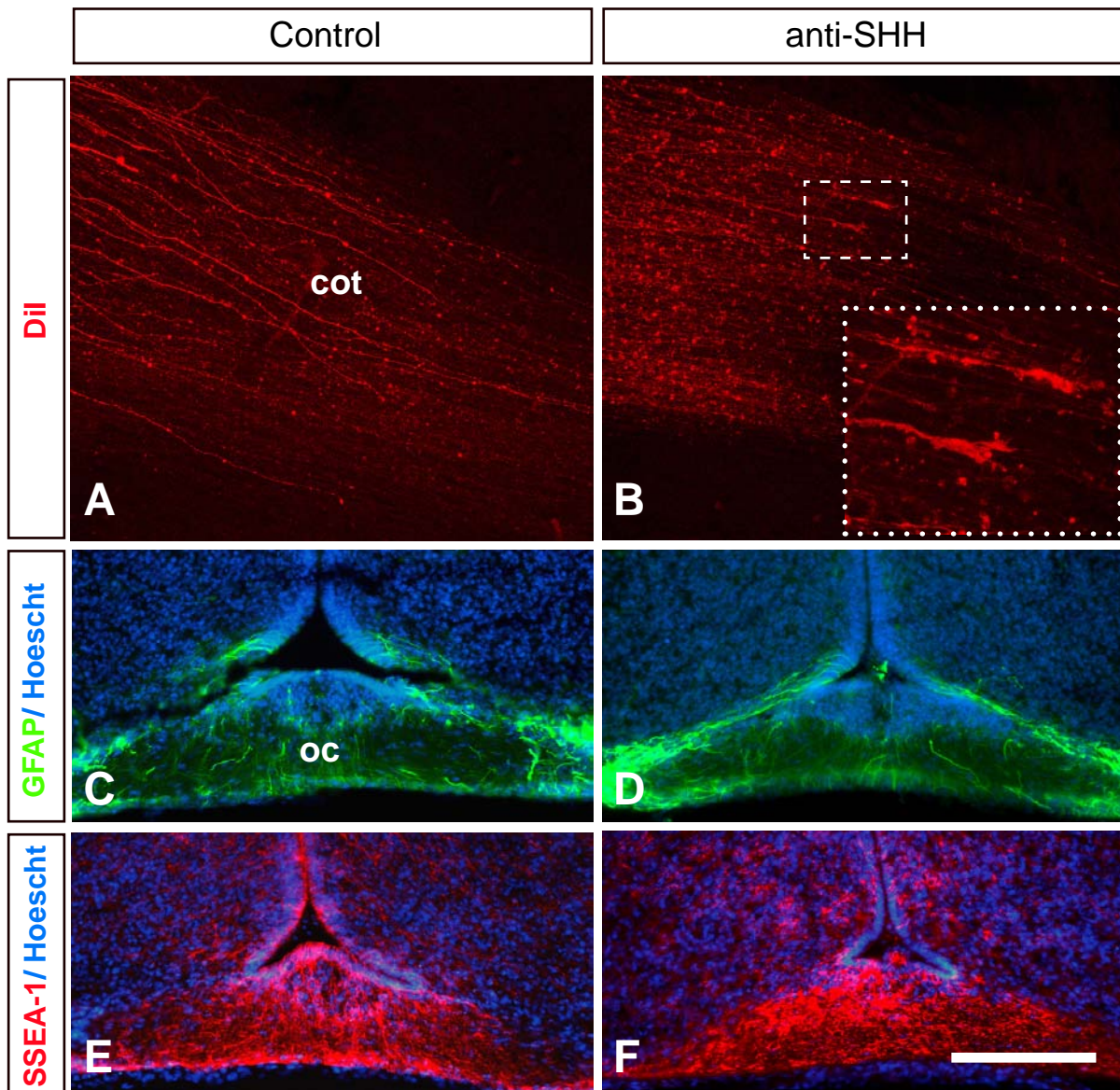
Supplementary material for this article is available at <http://dev.biologists.org/cgi/content/full/135/20/3531/DC1>

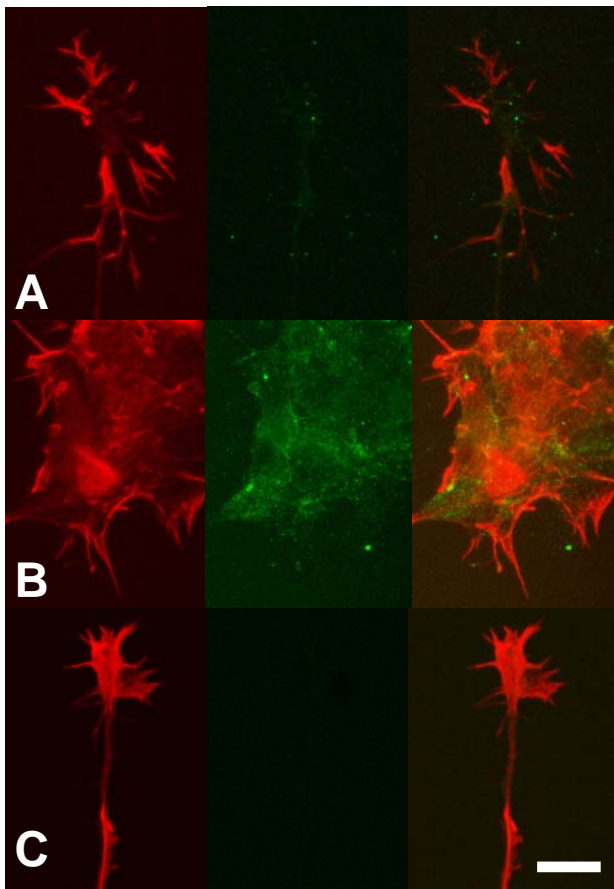
References

- Amato, M. A., Boy, S. and Perron, M. (2004). Hedgehog signaling in vertebrate eye development: a growing puzzle. *Cell. Mol. Life Sci.* **61**, 899-910.
- Barresi, M. J., Hutson, L. D., Chien, C. B. and Karlstrom, R. O. (2005). Hedgehog regulated Slit expression determines commissure and glial cell position in the zebrafish forebrain. *Development* **132**, 3643-3656.
- Bijlsma, M. F., Borensztajn, K. S., Roelink, H., Peppelenbosch, M. P. and Spek, C. A. (2007). Sonic hedgehog induces transcription-independent cytoskeletal rearrangement and migration regulated by arachidonate metabolites. *Cell Signal.* **19**, 2596-2604.
- Bourikas, D., Pekarik, V., Baeriswyl, T., Grunditz, A., Sadhu, R., Nardo, M. and Stoeckli, E. T. (2005). Sonic hedgehog guides commissural axons along the longitudinal axis of the spinal cord. *Nat. Neurosci.* **8**, 297-304.
- Bovolenta, P. and Mason, C. (1987). Growth cone morphology varies with position in the developing mouse visual pathway from retina to first targets. *J. Neurosci.* **7**, 1447-1460.
- Bovolenta, P., Rodriguez, J. and Esteve, P. (2006). Frizzled/Ryk mediated signalling in axon guidance. *Development* **133**, 4399-4408.
- Briscoe, J., Chen, Y., Jessell, T. M. and Struhl, G. (2001). A hedgehog-insensitive form of patched provides evidence for direct long-range morphogen activity of sonic hedgehog in the neural tube. *Mol. Cell* **7**, 1279-1291.
- Brown, L. Y., Kottmann, A. H. and Brown, S. (2003). Immunolocalization of Zic2 expression in the developing mouse forebrain. *Gene Expr. Patterns* **3**, 361-367.
- Butler, S. J. and Tear, G. (2007). Getting axons onto the right path: the role of transcription factors in axon guidance. *Development* **134**, 439-448.
- Casali, A. and Struhl, G. (2004). Reading the Hedgehog morphogen gradient by measuring the ratio of bound to unbound Patched protein. *Nature* **431**, 76-80.
- Charron, F., Stein, E., Jeong, J., McMahon, A. P. and Tessier-Lavigne, M. (2003). The morphogen sonic hedgehog is an axonal chemoattractant that collaborates with netrin-1 in midline axon guidance. *Cell* **113**, 11-23.
- Chuang, P. T. and McMahon, A. P. (1999). Vertebrate hedgehog signalling modulated by induction of a hedgehog-binding protein. *Nature* **397**, 617-621.
- Chung, K. Y., Taylor, J. S., Shum, D. K. and Chan, S. O. (2000). Axon routing at the optic chiasm after enzymatic removal of chondroitin sulfate in mouse embryos. *Development* **127**, 2673-2683.
- Culverwell, J. and Karlstrom, R. O. (2002). Making the connection: retinal axon guidance in the zebrafish. *Semin. Cell Dev. Biol.* **13**, 497-506.
- Dakubo, G. D., Wang, Y. P., Mazerolle, C., Campsall, K., McMahon, A. P. and Wallace, V. A. (2003). Retinal ganglion cell-derived sonic hedgehog signaling is required for optic disc and stalk neuroepithelial cell development. *Development* **130**, 2967-2980.
- de la Torre, J. R., Hopker, V. H., Ming, G. L., Poo, M. M., Tessier-Lavigne, M., Hemmati-Brivanlou, A. and Holt, C. E. (1997). Turning of retinal growth cones in a netrin-1 gradient mediated by the netrin receptor DCC. *Neuron* **19**, 1211-1224.
- Deshpande, G., Swanhart, L., Chiang, P. and Schedl, P. (2001). Hedgehog signaling in germ cell migration. *Cell* **106**, 759-769.
- Erskine, L. and Herrera, E. (2007). The retinal ganglion cell axon's journey: insights into molecular mechanisms of axon guidance. *Dev. Biol.* **308**, 1-14.
- Erskine, L., Williams, S. E., Brose, K., Kidd, T., Rachel, R. A., Goodman, C. S., Tessier-Lavigne, M. and Mason, C. A. (2000). Retinal ganglion cell axon guidance in the mouse optic chiasm: expression and function of robo and slits. *J. Neurosci.* **20**, 4975-4982.
- Esteve, P. and Bovolenta, P. (2006). Secreted inducers in vertebrate eye development: more functions for old morphogens. *Curr. Opin. Neurobiol.* **16**, 13-19.
- Frank-Kamenetsky, M., Zhang, X. M., Bottega, S., Guicherit, O., Wichterle, H., Dudek, H., Bumcrot, D., Wang, F. Y., Jones, S., Shulok, J. et al. (2002). Small-molecule modulators of Hedgehog signaling: identification and characterization of Smoothed agonists and antagonists. *J. Biol.* **1**, 10.
- Fucillo, M., Joyner, A. L. and Fishell, G. (2006). Morphogen to mitogen: the multiple roles of hedgehog signalling in vertebrate neural development. *Nat. Rev. Neurosci.* **7**, 772-783.
- García-Frigola, C., Carreres, M. I., Vegar, C. and Herrera, E. (2007). Gene delivery into mouse retinal ganglion cells by in utero electroporation. *BMC Dev. Biol.* **7**, 103.
- Gering, M. and Patient, R. (2005). Hedgehog signaling is required for adult blood stem cell formation in zebrafish embryos. *Dev. Cell* **8**, 389-400.
- Godement, P., Vanselow, J., Thanos, S. and Bonhoeffer, F. (1987). A study in developing visual systems with a new method of staining neurones and their processes in fixed tissue. *Development* **101**, 697-713.
- Gonzalez-Quevedo, R., Shoffer, M., Horg, L. and Oro, A. E. (2005). Receptor tyrosine phosphatase-dependent cytoskeletal remodeling by the hedgehog-responsive gene MIM/BEG4. *J. Cell Biol.* **168**, 453-463.
- Goodrich, L. V., Johnson, R. L., Milenkovic, L., McMahon, J. A. and Scott, M. P. (1996). Conservation of the hedgehog/patched signaling pathway from flies to mice: induction of a mouse patched gene by Hedgehog. *Genes Dev.* **10**, 301-312.
- Guerrero, I. and Chiang, C. (2007). A conserved mechanism of Hedgehog gradient formation by lipid modifications. *Trends Cell Biol.* **17**, 1-5.
- Hao, Y. L., Chan, S. O. and Dong, W. R. (2006). Changes of retinofugal pathway development in mouse embryos after Sonic hedgehog antibody perturbation. *Nan Fang Yi Ke Da Xue Xue Bao* **26**, 1679-1684.
- Harfe, B. D., Scherz, P. J., Nissim, S., Tian, H., McMahon, A. P. and Tabin, C. J. (2004). Evidence for an expansion-based temporal Shh gradient in specifying vertebrate digit identities. *Cell* **118**, 517-528.
- Hayhurst, M., Gore, B. B., Tessier-Lavigne, M. and McConnell, S. K. (2008). Ongoing sonic hedgehog signaling is required for dorsal midline formation in the developing forebrain. *Dev. Neurobiol.* **68**, 83-100.
- Herrera, E., Brown, L., Aruga, J., Rachel, R. A., Dolen, G., Mikoshiba, K., Brown, S. and Mason, C. A. (2003). Zic2 patterns binocular vision by specifying the uncrossed retinal projection. *Cell* **114**, 545-557.
- Hornberger, M. R., Dutting, D., Ciossek, T., Yamada, T., Handwerker, C., Lang, S., Weth, F., Huf, J., Wessel, R., Logan, C. et al. (1999). Modulation of EphA receptor function by coexpressed ephrinA ligands on retinal ganglion cell axons. *Neuron* **22**, 731-742.
- Inatani, M., Irie, F., Plump, A. S., Tessier-Lavigne, M. and Yamaguchi, Y. (2003). Mammalian brain morphogenesis and midline axon guidance require heparan sulfate. *Science* **302**, 1044-1046.
- Ingram, W. J., Wicking, C. A., Grimmond, S. M., Forrest, A. R. and Wainwright, B. J. (2002). Novel genes regulated by Sonic Hedgehog in pluripotent mesenchymal cells. *Oncogene* **21**, 8196-8205.
- Kapfhammer, J. P. and Raper, J. A. (1987). Collapse of growth cone structure on contact with specific neurites in culture. *J. Neurosci.* **7**, 201-212.
- Kato, K., Chihara, T. and Hayashi, S. (2004). Hedgehog and Decapentaplegic instruct polarized growth of cell extensions in the Drosophila trachea. *Development* **131**, 5253-5261.
- Kolpak, A., Zhang, J. and Bao, Z. Z. (2005). Sonic hedgehog has a dual effect on the growth of retinal ganglion axons depending on its concentration. *J. Neurosci.* **25**, 3432-3441.
- Lin, L. and Chan, S. O. (2003). Perturbation of CD44 function affects chiasmatic routing of retinal axons in brain slice preparations of the mouse retinofugal pathway. *Eur. J. Neurosci.* **17**, 2299-2312.
- Macdonald, R., Barth, K. A., Xu, Q., Holder, N., Mikkola, I. and Wilson, S. W. (1995). Midline signalling is required for Pax gene regulation and patterning of the eyes. *Development* **121**, 3267-3278.

- Manning, L., Ohya, K., Saeger, B., Hatano, O., Wilson, S. A., Logan, M. and Placzek, M.** (2006). Regional morphogenesis in the hypothalamus: a BMP-Tbx2 pathway coordinates fate and proliferation through Shh downregulation. *Dev. Cell* **11**, 873-885.
- Marcus, R. C. and Mason, C. A.** (1995). The first retinal axon growth in the mouse optic chiasm: axon patterning and the cellular environment. *J. Neurosci.* **15**, 6389-6402.
- Marcus, R. C., Shimamura, K., Sretavan, D., Lai, E., Rubenstein, J. L. and Mason, C. A.** (1999). Domains of regulatory gene expression and the developing optic chiasm: correspondence with retinal axon paths and candidate signaling cells. *J. Comp. Neurol.* **403**, 346-358.
- Martinez-Morales, J. R., Del Bene, F., Nica, G., Hammerschmidt, M., Bovolenta, P. and Wittbrodt, J.** (2005). Differentiation of the vertebrate retina is coordinated by an FGF signaling center. *Dev. Cell* **8**, 565-574.
- Mason, C. A. and Sretavan, D. W.** (1997). Glia, neurons, and axon pathfinding during optic chiasm development. *Curr. Opin. Neurobiol.* **7**, 647-653.
- Merchan, P., Bribian, A., Sanchez-Camacho, C., Lezameta, M., Bovolenta, P. and de Castro, F.** (2007). Sonic hedgehog promotes the migration and proliferation of optic nerve oligodendrocyte precursors. *Mol. Cell. Neurosci.* **36**, 355-368.
- Ming, G. L., Wong, S. T., Henley, J., Yuan, X. B., Song, H. J., Spitzer, N. C. and Poo, M. M.** (2002). Adaptation in the chemotactic guidance of nerve growth cones. *Nature* **417**, 411-418.
- Morcillo, J., Martinez-Morales, J. R., Trousse, F., Fermin, Y., Sowden, J. C. and Bovolenta, P.** (2006). Proper patterning of the optic fissure requires the sequential activity of BMP7 and SHH. *Development* **133**, 3179-3190.
- Nakagawa, S., Brennan, C., Johnson, K. G., Shewan, D., Harris, W. A. and Holt, C. E.** (2000). Ephrin-B regulates the ipsilateral routing of retinal axons at the optic chiasm. *Neuron* **25**, 599-610.
- Niclou, S. P., Jia, L. and Raper, J. A.** (2000). Slit2 is a repellent for retinal ganglion cell axons. *J. Neurosci.* **20**, 4962-4974.
- Okada, A., Charron, F., Morin, S., Shin, D. S., Wong, K., Fabre, P. J., Tessier-Lavigne, M. and McConnell, S. K.** (2006). Boc is a receptor for sonic hedgehog in the guidance of commissural axons. *Nature* **444**, 369-373.
- Pak, W., Hindges, R., Lim, Y. S., Pfaff, S. L. and O'Leary, D. D.** (2004). Magnitude of binocular vision controlled by islet-2 repression of a genetic program that specifies laterality of retinal axon pathfinding. *Cell* **119**, 567-578.
- Pearse, R. V., 2nd, Vogan, K. J. and Tabin, C. J.** (2001). Ptc1 and Ptc2 transcripts provide distinct readouts of Hedgehog signaling activity during chick embryogenesis. *Dev. Biol.* **239**, 15-29.
- Piper, M., Salih, S., Weinl, C., Holt, C. E. and Harris, W. A.** (2005). Endocytosis-dependent desensitization and protein synthesis-dependent resensitization in retinal growth cone adaptation. *Nat. Neurosci.* **8**, 179-186.
- Placzek, M. and Briscoe, J.** (2005). The floor plate: multiple cells, multiple signals. *Nat. Rev. Neurosci.* **6**, 230-240.
- Plump, A. S., Erskine, L., Sabatier, C., Brose, K., Epstein, C. J., Goodman, C. S., Mason, C. A. and Tessier-Lavigne, M.** (2002). Slit1 and Slit2 cooperate to prevent premature midline crossing of retinal axons in the mouse visual system. *Neuron* **33**, 219-232.
- Pratt, T., Conway, C. D., Tian, N. M., Price, D. J. and Mason, J. O.** (2006). Heparan sulphation patterns generated by specific heparan sulfotransferase enzymes direct distinct aspects of retinal axon guidance at the optic chiasm. *J. Neurosci.* **26**, 6911-6923.
- Ringstedt, T., Braisted, J. E., Brose, K., Kidd, T., Goodman, C., Tessier-Lavigne, M. and O'Leary, D. D.** (2000). Slit inhibition of retinal axon growth and its role in retinal axon pathfinding and innervation patterns in the diencephalon. *J. Neurosci.* **20**, 4983-4991.
- Rosentreter, S. M., Davenport, R. W., Loschinger, J., Huf, J., Jung, J. and Bonhoeffer, F.** (1998). Response of retinal ganglion cell axons to striped linear gradients of repellent guidance molecules. *J. Neurobiol.* **37**, 541-562.
- Sanchez-Camacho, C., Rodriguez, J., Ruiz, J. M., Trousse, F. and Bovolenta, P.** (2005). Morphogens as growth cone signalling molecules. *Brain Res. Brain Res. Rev.* **49**, 242-252.
- Tenzen, T., Allen, B. L., Cole, F., Kang, J. S., Krauss, R. S. and McMahon, A. P.** (2006). The cell surface membrane proteins Cdo and Boc are components and targets of the Hedgehog signaling pathway and feedback network in mice. *Dev. Cell* **10**, 647-656.
- Testaz, S., Jarov, A., Williams, K. P., Ling, L. E., Koteliansky, V. E., Fournier-Thibault, C. and Duband, J. L.** (2001). Sonic hedgehog restricts adhesion and migration of neural crest cells independently of the Patched-Smoothed-Gli signaling pathway. *Proc. Natl. Acad. Sci. USA* **98**, 12521-12526.
- Torres, M., Gomez-Pardo, E. and Gruss, P.** (1996). Pax2 contributes to inner ear patterning and optic nerve trajectory. *Development* **122**, 3381-3391.
- Traiffort, E., Moya, K. L., Faure, H., Hassig, R. and Ruat, M.** (2001). High expression and anterograde axonal transport of aminoterminal sonic hedgehog in the adult hamster brain. *Eur. J. Neurosci.* **14**, 839-850.
- Trousse, F., Marti, E., Gruss, P., Torres, M. and Bovolenta, P.** (2001). Control of retinal ganglion cell axon growth: a new role for Sonic hedgehog. *Development* **128**, 3927-3936.
- Van Horck, F. P. and Holt, C. E.** (2008). A cytoskeletal platform for local translation in axons. *Sci. Signal.* **1**, pe11.
- Vokes, S. A., Yatskevych, T. A., Heimark, R. L., McMahon, J., McMahon, A. P., Antin, P. B. and Krieg, P. A.** (2004). Hedgehog signaling is essential for endothelial tube formation during vasculogenesis. *Development* **131**, 4371-4380.
- Wallace, V. A. and Raff, M. C.** (1999). A role for Sonic hedgehog in axon-to-astrocyte signalling in the rodent optic nerve. *Development* **126**, 2901-2909.
- Wang, Y., Dakubo, G. D., Thurig, S., Mazerolle, C. J. and Wallace, V. A.** (2005). Retinal ganglion cell-derived sonic hedgehog locally controls proliferation and the timing of RGC development in the embryonic mouse retina. *Development* **132**, 5103-5113.
- Williams, S. E., Mann, F., Erskine, L., Sakurai, T., Wei, S., Rossi, D. J., Gale, N. W., Holt, C. E., Mason, C. A. and Henkemeyer, M.** (2003). Ephrin-B2 and EphB1 mediate retinal axon divergence at the optic chiasm. *Neuron* **39**, 919-935.
- Williams, S. E., Grumet, M., Colman, D. R., Henkemeyer, M., Mason, C. A. and Sakurai, T.** (2006). A role for Nr-CAM in the patterning of binocular visual pathways. *Neuron* **50**, 535-547.
- Wirth, M. J., Brun, A., Grabert, J., Patz, S. and Wahle, P.** (2003). Accelerated dendritic development of rat cortical pyramidal cells and interneurons after biolistic transfection with BDNF and NT4/5. *Development* **130**, 5827-5838.







EGFP + anti-SHH

